Proceedings of the DIS'2004, Štrbské Pleso, Slovakia

ELASTIC AND DIFFRACTIVE SCATTERING AT DØ

TAMSIN EDWARDS
(FOR THE DØ COLLABORATION)
Department of Physics & Astronomy, University of Manchester, Oxford Road, M13 9PL, UK
E-mail: tamsin@fnal.gov

The first search for diffractively produced Z bosons in the muon decay channel is presented, using a data set collected by the DØ detector at the Fermilab Tevatron at $\sqrt{s} = 1.96$ TeV between April and September 2003, corresponding to an integrated luminosity of approximately 110 pb^{-1}. The first $dN/d|t|$ distribution for proton-antiproton elastic scattering at the Fermilab Tevatron is also presented, using data collected by the DØ Forward Proton Detector between January and May 2002. The measured slope is reproduced by theoretical predictions.

1 Introduction

QCD models elastic and single diffractive scattering of hadrons as proceeding via the exchange of a colour singlet object. In the case of elastic proton-antiproton scattering, both protons[a] emerge intact and scattered at a small angle, with no momentum loss and no other particles produced. In single diffraction, where one proton remains intact with a small momentum loss and the other dissociates, there may be an area devoid of activity (rapidity gap) in the region of the outgoing intact proton. We present here the first ever search for diffractively produced Z bosons in the muon decay channel and the first measurement of elastic scattering as a function of four-momentum transfer squared at the Fermilab Tevatron.

2 Diffractive Z boson production

2.1 Event selection and data analysis

Z bosons produced via single diffraction are identified by demanding a rapidity gap near the beampipe in either the outgoing proton or antiproton direction. The data set was collected between April and September 2003 by the DØ detector at the Fermilab Tevatron, corresponding to an integrated luminosity of approximately 110 pb^{-1}. The DØ detector is described in detail elsewhere [1]. The Z boson is selected via its decay into two oppositely charged muons each with $p_T > 15$ GeV. At least one muon must be isolated in the central tracking detector and the calorimeter: Σp_T of tracks within a cone of radius 0.5 around the muon is required to be less than 3.5 GeV, and in the calorimeter (ΣE_T in a cone of radius of 0.5 around the muon) - (ΣE_T in a cone of radius of 0.1 around the muon) is required to be less than

[a]Here the term 'proton' is used to refer to both protons and antiprotons.

2.5 GeV, where the cone radius is defined in pseudorapidity η and azimuthal angle ϕ as $\Delta R = \sqrt{\Delta\eta^2 + \Delta\phi^2}$. Cosmic ray muon events are vetoed by requiring that the distance of closest approach of muon tracks to the beam position is less than 0.02 cm for tracks with hits in both the Silicon Micro-vertex Tracker (SMT) and Central Fiber Tracker (CFT), or less than 0.2 cm for tracks with hits only in the CFT. In addition, the muon tracks are required to fulfil $|\Delta\phi_{\mu\mu} + \Delta\theta_{\mu\mu} - 2\pi| > 0.05$ radians, where θ is polar angle.

The rapidity gap search makes use of two detectors, the Luminosity Monitor (LM) and the end calorimeter. The LM comprises two scintillating detectors, one on each side of the interaction region, which cover the pseudorapidity range $2.7 < |\eta| < 4.4$. The total output charge is discriminated to give an on/off signal for each detector. The end calorimeter is divided into three regions: (1) four electromagnetic layers closest to the beam, (2) four fine hadronic layers and (3) one coarse hadronic layer furthest from the beam. Each layer is divided into cells in the $\eta - \phi$ plane. For this analysis, the energy is summed separately on each side (outgoing proton and antiproton) in the range $2.6 < |\eta| < 5.3$, using electromagnetic cells with $E_{\mathrm{cell}} > 100$ MeV and fine hadronic cells with $E_{\mathrm{cell}} > 200$ MeV.

The log of the energy sum on the outgoing antiproton side is plotted in Figure 1 for bunch crossings in which there are no visible interactions. These are selected from a randomly triggered sample with the requirements that both LM detectors are off and there is no vertex with greater than two associated tracks. These events are used to approximate rapidity gap events, in which there is no activity in the outgoing antiproton direction. The log of the energy sum on the outgoing antiproton side is also shown for a sample of minimum bias events in the figure. These are selected requiring hits in both detectors of the LM within a small time window. A third (25 GeV jet) sample is selected by requiring a vertex with at least three tracks, and at least one jet with $p_T > 25$ GeV that passes jet quality cuts. Jet events in which the highest p_T jet lies in the region $|\eta| > 2.4$ are excluded. The minimum bias and jet samples are dominated by events in which both protons dissociate.

Events with no interaction and events with antiproton dissociation are separated by applying a cut at an energy sum of 10 GeV. This is also the case in the outgoing proton direction. To select single diffractive candidates in the Z boson sample the LM detector is required to be off and the energy sum less than 10 GeV on one side, and the LM detector is required to be on and the energy sum greater than 10 GeV on the other side.

2.2 Results

Figure 2 shows the di-muon invariant mass distribution for two samples. Fig. 2(a) shows those events that fail the two rapidity gap cuts on both the outgoing proton and antiproton sides. These are strong candidates for non-diffractive production of Z bosons. A resonant peak is observed together with a small background contribution, arising mainly from the $(Z/\gamma)^*$ continuum. Fig. 2(b) shows those events that pass both rapidity gap cuts on one side and fail both on the other. These are candidates for single diffractively produced Z bosons, where one proton is intact

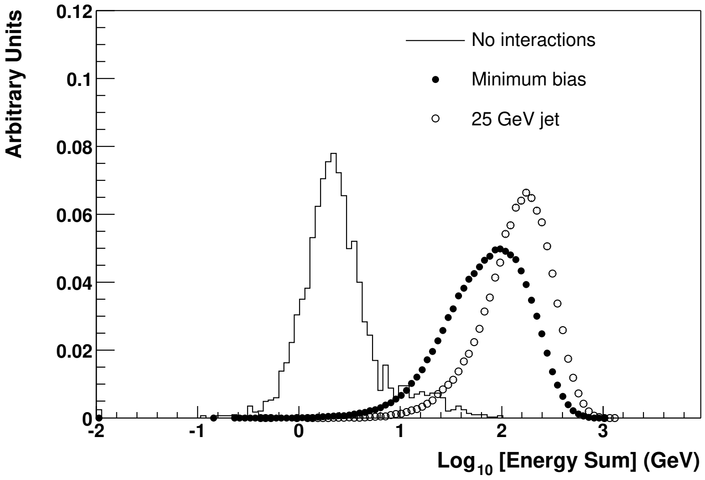

Figure 1. Log of energy sum in the outgoing antiproton direction ($-5.3 < \eta < -2.6$), comparing events with no visible interactions with events in which both protons dissociate. Areas are normalised to unity. An energy sum cut is applied at 10 GeV for rapidity gap candidates.

and the other dissociates.

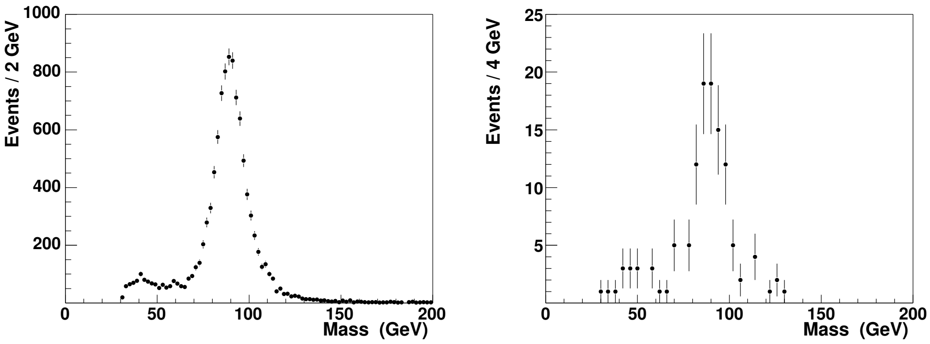

(a) No rapidity gap

(b) Single rapidity gap

Figure 2. The di-muon invariant mass distribution for Z boson candidates with (a) no rapidity gap and (b) a single rapidity gap. A rapidity gap is defined as one LM detector off and energy sum less than 10 GeV in the same region (see text for details).

3 Elastic scattering

3.1 Event selection and data analysis

Elastic scattering can be reconstructed at DØ using the Forward Proton Detector (FPD), a series of momentum spectrometers that make use of accelerator magnets in conjunction with position detectors along the beam line [2]. In total the FPD has nine spectrometers, each comprising two scintillating fibre tracking detectors that can be moved to within a few millimetres of the beam. Reconstructed track four vectors are used to calculate the kinematic variables of scattered protons: t, the four-momentum transfer squared, and ξ, the fractional longitudinal momentum loss. The data for this analysis were collected between January and May 2002. Two spectrometers were used to trigger elastic events: one above the beam on the outgoing antiproton side, and the other below the beam on the opposite outgoing proton side. The latter is used here for track position measurement. The trigger makes use of time-of-flight information, and vetoes events with hits in the LM or hits in the Veto Counters (covering the pseudorapidity range $5.2 < |\eta| < 5.9$). The spectrometers are preceded by quadrupole (focusing) accelerator magnets, and can reconstruct protons at any ξ value and in the kinematic range $0.8 \lesssim |t| \lesssim 4.0$ GeV^2, depending on detector position and accelerator conditions. The measurement presented here covers the range $0.92 < |t| < 1.34$ GeV^2.

A custom-written Monte Carlo event generator is used to model the hits which outgoing elastically scattered protons leave in the detectors after they have propagated through the Tevatron magnetic field lattice [3]. The estimated detector resolution is included, and the $dN/d|t|$ distribution of elastic scattering events is assumed to decrease exponentially with increasing $|t|$. A similar event generator [4] is used to model the detector geometric acceptance as a function of $|t|$. Elastically scattered particles have near-zero measured momentum loss, and hit the first and second detectors at almost equal positions in the $x - y$ plane. Tracks outside this region are expected to originate mostly from single diffractive events or halo (beam loss) particles, and are excluded.

Halo and diffractive particles that contribute to the signal region of the detector are subtracted. For halo, the $dN/d|t|$ distribution and fraction of events in the signal region are modelled by the Fermilab Accelerator Division [5]. This is normalised using the number of events excluded from the signal region, assuming that all the excluded events with $|\xi| < 0.03$ are halo. For single diffractive events, the $dN/d|t|$ distribution is taken from excluded events with $|\xi| > 0.03$. The normalisation assumes that the probability for a diffractive proton to hit the detector is constant everywhere over the detector surface: this estimate is used to subtract the contribution inside the signal region.

An unsmearing correction is also applied to the data sample to account for the effect of detector resolution.

3.2 Results

Figure 3 shows the measured (and corrected) $dN/d|t|$ distribution for elastic proton-antiproton scattering. The DØ data are shown alongside $d\sigma/d|t|$ measurements from other experiments at different centre of mass energies [6]. The normalisation of the new data is arbitrary. The slope is compared with the theoretical prediction of Block *et al.* [7]. The model is able to reproduce the data, which show a change in slope between the high and low $|t|$ regions.

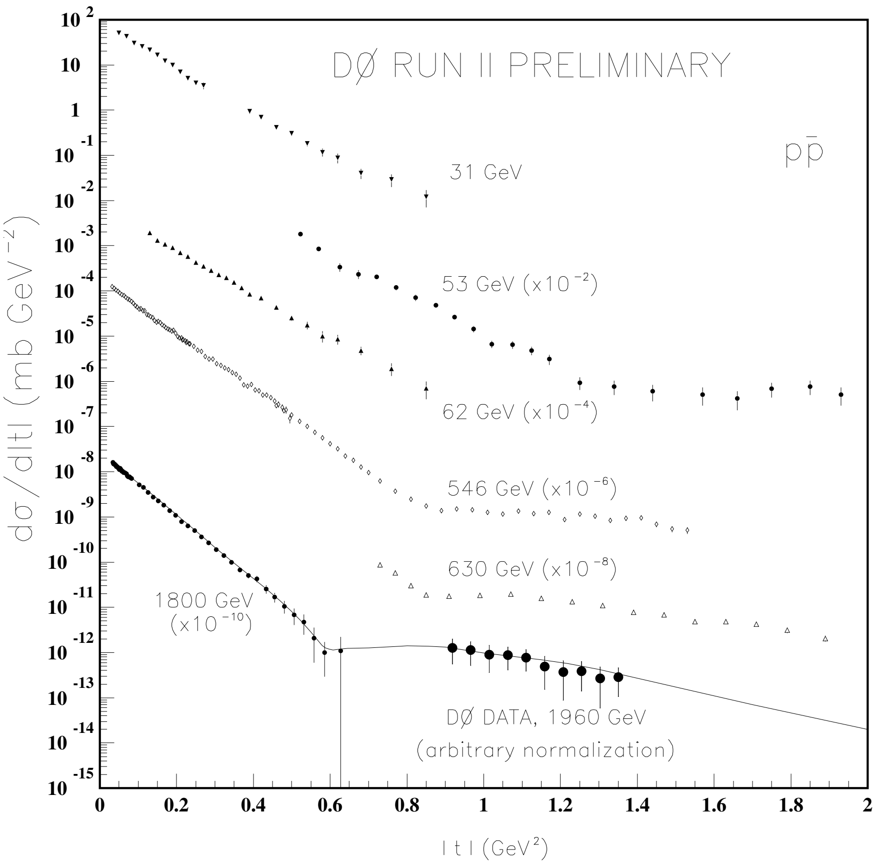

Figure 3. Distributions of $d\sigma/d|t|$ for elastic scattering measured by various experiments [6]. The slope of the new DØ data is compared with the theoretical model of Block *et al.* [7]. The normalisation of the DØ points is arbitrary. The other data have been scaled for visual separation.

Summary

A search for diffractively produced Z bosons in the muon channel has been presented. The sample is large enough to allow a study of the kinematic properties of the Z bosons for the first time.

Proton-antiproton elastic scattering is measured for the first time at $\sqrt{s} = 1.96$ TeV, in the four-momentum transfer squared range $0.92 < |t| < 1.34$ GeV^2. The slope is reproduced by the predictions of Block *et al.*.

Acknowledgements

We thank the staffs at Fermilab and collaborating institutions, and acknowledge support from the Department of Energy and National Science Foundation (USA), Commissariat à l'Energie Atomique and CNRS/Institut National de Physique Nucléaire et de Physique des Particules (France), Ministry of Education and Science, Agency for Atomic Energy and RF President Grants Program (Russia), CAPES, CNPq, FAPERJ, FAPESP and FUNDUNESP (Brazil), Departments of Atomic Energy and Science and Technology (India), Colciencias (Colombia), CONACyT (Mexico), KRF (Korea), CONICET and UBACyT (Argentina), The Foundation for Fundamental Research on Matter (The Netherlands), PPARC (United Kingdom), Ministry of Education (Czech Republic), Natural Sciences and Engineering Research Council and WestGrid Project (Canada), BMBF (Germany), A.P. Sloan Foundation, Civilian Research and Development Foundation, Research Corporation, Texas Advanced Research Program, and the Alexander von Humboldt Foundation.

References

1. V. Abazov *et al.* (DØ collaboration), to be submitted to Nucl. Instrum. Methods A; T. LeCompte and H. T. Diehl, Ann. Rev. Nucl. Part. Sci. **50**, 71 (2000).
2. A. Brandt *et al.* (DØ collaboration), FERMILAB-PUB-97-377.
3. J. Molina and V. Oguri, Nov 2002. Available at: <http://alpha1.lafex.cbpf.br/~molina/elastic_mc/>
4. J. Barreto and J. Montanha, Jan 2003. Available at: <http://www.ifi.unicamp.br/~montanha/fpd/sources/quadrupoles/pot_ver.for>
5. A. I. Drozhdin *et al.*, FERMILAB-FN-0734.
6. A. Breakstone *et al.* [AMES-BOLOGNA-CERN-DORTMUND-HEIDELBERG-WARSAW Collaboration], Nucl. Phys. B **248**, 253 (1984);
   A. Breakstone *et al.*, Phys. Rev. Lett. **54**, 2180 (1985);
   R. Battiston *et al.* [UA4 Collaboration], Phys. Lett. B **127**, 472 (1983);
   M. Bozzo *et al.* [UA4 Collaboration], Phys. Lett. B **155**, 197 (1985);
   D. Bernard *et al.* [UA4 Collaboration], Phys. Lett. B **171**, 142 (1986);
   N. A. Amos *et al.* [E-710 Collaboration], Phys. Lett. B **247**, 127 (1990).
7. M. Block *et al.*, Phys. Rev. D **41**, 978 (1990).